Journal of Computational Electronics (2020) 19:310–320
https://doi.org/10.1007/s10825-019-01429-w

# Design and simulation of a high sensitive stripped-shaped piezoresistive pressure sensor

**Maliha Farhath**[1] · **Mst. Fateha Samad**[1]

Published online: 10 December 2019


**Abstract**
This paper deals with the design and simulation of a stripped-shaped piezoresistive pressure sensor. The sensor is based on the Wheatstone bridge configuration. The piezoresistive effect is a change in the electrical resistivity of a semiconductor or metal when mechanical strain is applied. For designing the sensor, piezoresistors are placed in series on each side of the square. The number of the piezoresistor arms is varied in two proposed designs where the sensitivity and the operable pressure range are analyzed with their characteristics. The COMSOL Multiphysics software is used for this work. The simulated sensitivity is about 7.736 mV/V/MPa over the range of pressure from 0 to 5 MPa. The simulated result reveals that the sensitivity significantly depends on the placement of the resistors, combination of the materials, shape of diaphragm, and size of diaphragm.

**Keywords** Wheatstone bridge · Piezoresistive · Pressure sensor · Sensitivity · COMSOL

## 1 Introduction

Nowadays, pressure sensors play a vital role to address concerns with the environment. Pressure sensors are used in different applications such as biomedical, industrial, automotive, chemical, aerospace, and water treatment [1–4]. Some advantages of pressure sensors are their small size, low cost, ease of fabrication, high reliability, and less stray factors. Micro-pressure sensors have been classified as absolute [5, 6], differential [7–9], and gauge [10] sensors based on the method of sensing. Micro-pressure sensors can also be categorized based on the mechanism of the transduction such as piezoresistive [11, 12], optical resonant [13, 14], and thermal sensors [15, 16].

Due to the emergence of microelectromechanical systems (MEMS), many kinds of MEMS-based pressure sensors have been invented. According to the sensing principles, MEMS-based pressure sensors can be divided into piezoresistive [17, 18], capacitive [19, 20], resonant [21], and so on. Among them, the piezoresistive MEMS pressure sensors are the most used one because of their significant advantages such as high sensitivity [22, 23], excellent linearity [23], and repeatability. The piezoresistive MEMS sensors operate through the change in electrical resistance by an external force applied to a semiconductor. This change only affects the material's electrical resistivity.

Recently, research on piezoresistive pressure sensor has been conducted. For instance, Hong et al. [24] designed an inner diaphragm of the piezoresistive pressure sensor. Their proposed model was compared with the original model. The proposed model had a square diaphragm with side of 1 mm and thickness of 20 µm. The model showed 13% increment in the sensitivity without decreasing the linearity. The achieved sensitivity was about − 6.02 mV/kpa. Moreover, Meti et al. [22] proposed silicon-based micro-pressure sensor where different configurations of p-type meander-shaped piezoresistors were used. The resistors were placed at the high strain region of the diaphragm surface with the configuration of Wheatstone bridge. The material used for the connecting arms was copper. It was mentioned that the sensitivities for 100 µm and 50 µm length of piezoresistors were 1.64 mV/kpa and 2.36 mV/kpa, respectively. In another simulation-based study, a silicon-based piezoresistive pressure sensor with meander-shaped piezoresistors was explored for the pressure range of 0 to 1 MPa [25]. The dimension of the designed sensor was 500 µm in width, 500 µm in depth, and

✉ Maliha Farhath
mfmridanka2906@gmail.com

Mst. Fateha Samad
fatehaeteruet@gmail.com

[1] Department of Electronics & Telecommunication Engineering, Rajshahi University of Engineering & Technology, Kazla, Rajshahi 6204, Bangladesh

10 µm in height. It also used copper as the metal strip to connect the piezoresistors. In this work, four different configurations of meander-shaped piezoresistive pressure sensors were analyzed. High sensitivity of 32.93 µV/V/Pa for two turn configurations and a high linearity for zero turn configurations were obtained. On the other hand, a pressure sensor based on the piezoresistive effect of graphene was presented by Zhu et al. [26]. The sensor used a square-shaped silicon nitride membrane which was 100 nm thick and 280 µm wide. The polycrystalline graphene piezoresistors were placed on the maximum strain area of the diaphragm. At the pressure range of 0–70 kPa, the diaphragm was deflected and the output voltage was produced. The achieved gauge factor for graphene was as 1.6. Similarly, a thin graphene-based MEMS intracranial piezoresistive pressure (ICP) sensor was introduced in [17]. The effect of residual stress on the graphene diaphragm was studied in the paper. It was found that 20 layers of graphene can reduce the residual stress on the diaphragm from $1.94\times10^{7}$ Mpa to $9.72\times10^{3}$ Mpa. Furthermore, a structural four-beams-bossed-membrane (FBBM) piezoresistive pressure sensor was invented in [27]. The performance of the stress distribution on sensitive elements and the deflection of membrane were examined using the finite element analysis. The relationships between the mechanical performance and dimension variables were determined, which provided an instruction for designing a sensor with FBBM structure. The results demonstrated a high sensitivity of 4.71 mV/V/kPa and a low pressure nonlinearity of 0.75% FSS. It also indicated that this novel structure-based sensor was a perfect sensor for working under 5 kPa. In addition, Guan et al. [28] reported a novel high sensitivity- and linearity-based piezoresistive pressure sensor. The design was analyzed using 0–3 kPa to determine the stress on the beam edge and the diaphragm deflection. A shuriken-structured diaphragm was fabricated which not only improves the sensitivity but also enhances the linearity performance of this piezoresistive pressure sensor. The fabricated sensor illustrated 4.72 mV/kPa/V of sensitivity and 0.18% FSO (full-scale output) of nonlinearity.

Overall, it is found that the piezoresistive pressure sensor mainly consists of silicon diaphragm with piezoresistive elements mounted on it. Silicon works as the sensing element, and semiconductors and metals work as piezoresistive materials. However, semiconductors are more preferred over the metals, since semiconductors exhibit higher gauge factor [29]. Widely used piezoresistive materials are polysilicon [30], polycrystalline SiC [31], single-crystal silicon carbide [32], carbon nanotubes [12], etc. In this design, the placement of the piezoresistors is selected in the form of Wheatstone bridge circuit. Wheatstone bridge circuit is used in piezoresistive pressure sensor because of the extreme accuracy. The Wheatstone bridge circuit determines the concept of the measurement of small differences, which shows the extreme accuracy. There are number of piezoresistor arms, which are placed on the diaphragm of the piezoresistive pressure sensor as the configuration of Wheatstone bridge circuit. Therefore, the change in resistance is measured simultaneously with the change in electric potential when the pressure is imposed on the surface of the piezoresistive pressure sensor. Moreover, the sensitivity of the bridge with four active arms is higher than any one or two active arms [33]. For this reason, Wheatstone bridge circuit is chosen as the basic principle of this piezoresistive pressure sensor. Having all these considerations, the sensitivity is achieved higher and the operable pressure range is much wider.

## 2 Theory

Piezoresistive pressure sensor works based on the piezoresistive effect. When the pressure sensor is subjected to the mechanical strain, the effective mass of silicon atoms either increases or decreases which in turn changes the mobility of the silicon carriers; hence, the resistance ($R$) of the material changes according to the following equation:

$$R = \rho l/A \tag{1}$$

where $A$ is the cross-sectional area of the piezoresistive material, $l$ is the length of the piezoresistive material, and $\rho$ is the resistivity of the material. Two important factors of piezoresistive pressure sensor are: the substrate of the sensor with a known area $A$ and the ingredient of the sensor. The sensor will respond to the applied force $F$, which is satisfied by the mathematical formula of pressure [34]. The pressure is related to the differential of force over area as:

$$P = \frac{\mathrm{d}F}{\mathrm{d}A} \tag{2}$$

The placement of the piezoresistors on the pressure sensor is arranged as the Wheatstone bridge circuit as shown in Fig. 1. In this circuit, there are four active arms. When there is a change in pressure, the two resistors $R1$ and $R3$ undergo a resistance change. This change in resistance is equal and opposite to the resistance change in $R2$ and $R4$. As a result,

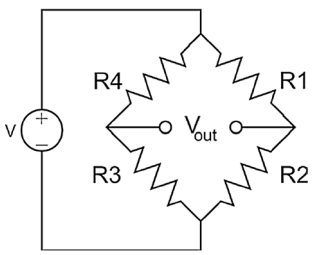


**Fig. 1** Wheatstone bridge circuit

the sensitivity of four active arms is higher than any one or two active arms. For this reason, Wheatstone bridge circuit configuration is considered [35].

When the pressure is applied to the diaphragm, it gets deformed. The quantity of displacement is measured at the center of the diaphragm using the following equation [11]:

$$D = 0.0151(1 - v^2)\frac{Pa^4}{Eh^3} \tag{3}$$

where $P$ is the applied pressure, $a$ is the side length of the diaphragm, $E$ is the Young's modulus, $h$ is the thickness of the diaphragm, and $v$ is the Poisson's ratio. The output voltage of the circuit depends on the input voltage and the applied pressure. This output voltage of the Wheatstone bridge circuit is given by [12]:

$$V_{\text{out}} = V_{\text{in}}\left[\frac{R2R3 - R1R4}{(R1 + R2)(R3 + R4)}\right] \tag{4}$$

Output voltage across Wheatstone bridge circuitry is measured analytically by using another equation [12]:

$$V_{\text{out}} = \frac{0.75Pa^2(1 - v)\pi_t V_{\text{in}}}{h^2} \tag{5}$$

where $\pi_t$ is the piezoresistive coefficient for transverse position and $V_{\text{in}}$ is the input voltage in $V$. The sensitivity of a pressure sensor is defined as the ratio of change in the output voltage to the change in the applied pressure with the input voltage. Mathematically it is defined by [36]:

$$\text{sensitivity} = \frac{\Delta V}{\Delta P} \cdot \frac{1}{V_{\text{in}}} \tag{6}$$

## 3 Design considerations

While designing a piezoresistive pressure sensor, there are some factors that must be kept into the considerations. First consideration is the selection of piezoresistive materials. Widely used piezoresistive materials are silicon [11], polysilicon [37], silicon di-oxide [28], carbon nanotube [12], graphene [26], etc. Therefore, the choice of material is an important matter because it results the change in the output of the sensor. The placement of the resistors is also a matter of consideration [11]. In the time of dimensioning the sensor, the thickness of the diaphragm is highly considered to obtain the best output characteristics from the sensor [38]. By maintaining these considerations, the proposed sensor is designed.

### 3.1 Materials used for the proposed designs

In this work, the selected piezoresistive material is silicon. However, depending on the application, different types of silicon materials can be used as piezoresistive element such as p-type and n-type silicon semiconductors. Moreover, there are some piezoresistive materials such as graphene and carbon nanotube (cnt) that have widely been used in other applications [12, 39]. In the proposed design, n-type silicon (single crystal, lightly doped) is used as diaphragm and p-type silicon (single crystal, lightly doped) is preferred for the resistors. For the connectors, metal can be used because it cannot affect the piezoresistive effect. However, the widely used materials for the connectors are silicon, copper, aluminum, etc. [22, 40]. In this design, silicon is also chosen as the connectors which might raise the performance [11, 22]. The properties of the materials used in this work are given in Table 1.

### 3.2 Placement of the resistors

For the enhancement of the sensitivity, the piezoresistors are needed to be placed properly. The optimal location to place the piezoresistive material would be the region of maximum strain on the diaphragm which is the four-edge side of the square diaphragm [11]. The application of pressure underneath the sensor causes a deflection of the diaphragm, and this causes a change in resistance hence change in the output voltage. The two resistors are placed in a way to experience the tensile strength which increases the resistance. Another two piezoresistors experience the decrease in the resistance. This proper placement of resistors also compensates the temperature compensation. Thus, the calculation of strain distribution and deflection with the change in the applied pressure becomes pivotal [11].

**Table 1** Properties of materials

| Properties | Material of diaphragm (n-type silicon) | Material of piezoresistors (p-type silicon) | Material of connectors (silicon) |
|---|---|---|---|
| Young's modulus [GPa] | 160 | 160 | |
| Poisson's ratio | 0.22 | 0.22 | |
| Density [kg/m$^3$] | 2330 | 2330 | |
| Electrical conductivity [S/m] | | | 1000 |

### 3.3 Diaphragm dimension of the proposed design

The thickness and the size of the diaphragm are a matter of consideration in designing the piezoresistive pressure sensor. The thinner diaphragm increases the sensitivity [38]. However, the thicker diaphragm increases the linearity [38]. Emphasizing on the sensitivity, the thickness of the diaphragm is fixed to 10 μm. The diaphragm of the sensor will be said to be 'thin' if the ratio of the thickness of the diaphragm to the length of the diaphragm is less than 1/20 [41]. Since the selected thickness of the diaphragm is 10 μm, the length of the diaphragm should be at least $10 \times 20 = 200$ μm. For this design, the length of the diaphragm is fixed to 400 μm.

## 4 Design and simulation

The performance of the piezoresistive pressure sensor not only depends on the properties of the materials but also depends on the shape of the sensor, the placement of the resistors, the size of the resistors, the thickness of the diaphragm, etc. The Young's modulus of the piezoresistive material and the electrical conductivity of the connector's material play a vital role in the sensitivity of the piezoresistive pressure sensor. Additionally, the length of the resistors and the thickness of the diaphragm are of great importance [22]. Keeping these concepts under consideration, two designs are proposed below.

### 4.1 Stripped-shaped piezoresistive pressure sensor (Design-1)

In this work, the shape of the sensor is chosen as square because it has advantages over circular and rectangle shape. The advantages are: The induced stress is maximum at the edges; and the strain is positive over wide range [42]. The proposed model is designed in the COMSOL Multiphysics 4.4. The designed sensor includes three piezoresistor arms in each side which are placed on the square diaphragm. The selected dimension of the substrate and the diaphragm is 500 μm × 500 μm and 400 μm × 400 μm, respectively. The thickness of the diaphragm is chosen as 10 μm. For designing the resistors and the connectors, a work plane is created on the diaphragm from the COMSOL tool. Then, the 2D geometry of the resistors and connectors is designed on the work plane. The total dimension of each resistor is approximately 100 μm × 10 μm where 33.3 μm length of each piezoresistor arm is slotted. The space between these piezoresistor arms is kept as 35 μm. For the connectors, 10 μm width of semiconductor is used between piezoresistors. The connectors are united using Boolean operations of the COMSOL tool. Then, the novel stripped-shaped piezoresistors are ready to employ for the simulation. Figure 2 shows the structure of the proposed pressure sensor.

For the simulation of this model, COMSOL study tool is used. The physics that is used in the simulation is piezoresistive boundary current. The boundary load is defined on the diaphragm area. The input voltage of 5 V is applied to one corner terminal of the diaphragm, while the other corner terminal is ground connected. For better performance, extremely fine meshing technique is employed. The simulation is done by pressure range of 0 to 5 MPa with the step size of 0.25 MPa. In each step, the displacement and the output voltage are computed. For instance, the maximum deformation at 1 MPa is obtained as 2.64 μm. The simulated displacement at 1 MPa is shown in Fig. 3. The change in the resistance of piezoresistors causes the change in output voltage across the Wheatstone bridge circuitry. Figure 4a shows the electric potential distribution of Design-1. The potential distribution is produced by the continuous charge distribution. Input terminal shows the highest electric potential distribution of 5 V as marked by the red color, and the ground terminal shows the lowest electric potential indicated by the blue color. The output voltage of Design-1 is found as 39.28 mV to 194 mV for 1 MPa to 5 MPa applied pressure.

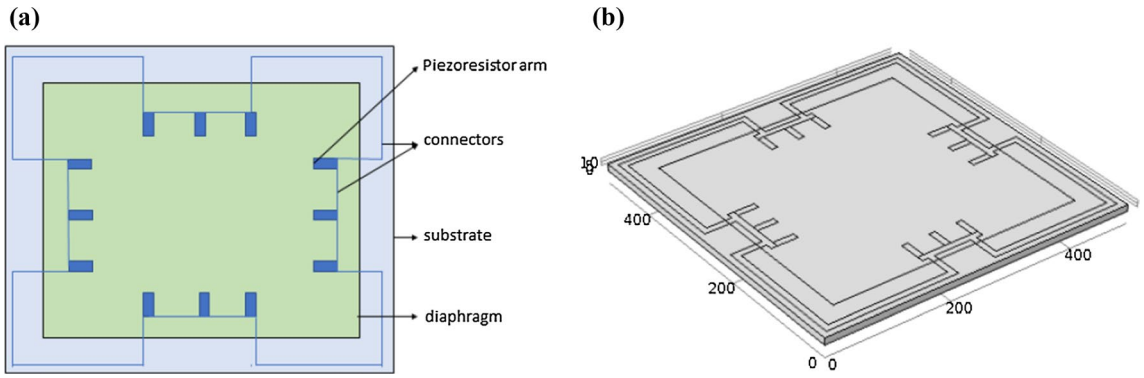


**Fig. 2** Pressure sensor of Design-1: **a** top view of the proposed model, **b** geometry designed in COMSOL

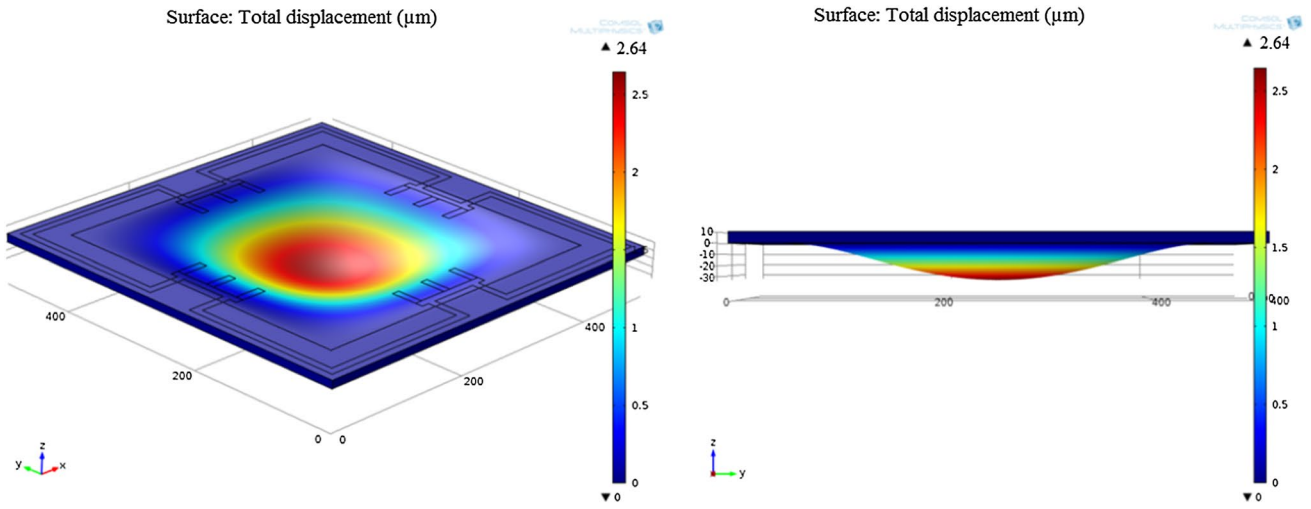


**Fig. 3** 3D simulation results of Design-1: total displacement is in µm range at the applied pressure of 1 MPa

Thus, output voltage increased with the increment in the applied pressure. Since the maximum operable pressure for Design-1 is 5 MPa, the highest obtained output voltage for Design-1 is 194 mV.

The stress region of the pressure sensor is simulated in a 3D plot. As shown in Fig. 4b, the high stress region lies on the area of the resistors. In this figure, the red area represents the maximum stress area where the resistors are located. The maximum stress is found as $8.97 \times 10^8$ N/m$^2$. This result is obtained by the expression of the first principle stress. The first principle stress is the maximum tensile stress induced in that area where the pressure is applied. Moreover, the maximum or ultimate tensile strength is the maximum applied pressure divided by the cross-sectional area where the pressure is applied. Using the maximum applied pressure of 5 MPa and the cross-sectional area of 400 µm × 10 µm, the ultimate tensile strength is found as $1250 \times 10^6$ MPa. The first principle stress of $8.97 \times 10^8$ N/m$^2$ does not exceed the ultimate tensile strength. This indicates Design-1 is optimized well and compatible for practical applications [43, 44].

## 4.2 Stripped-shaped piezoresistive pressure sensor (Design-2)

In this model, the shape and size of the sensor are same as previous design. The main difference from Design-1 is the number of the piezoresistor arms. In this design, there are

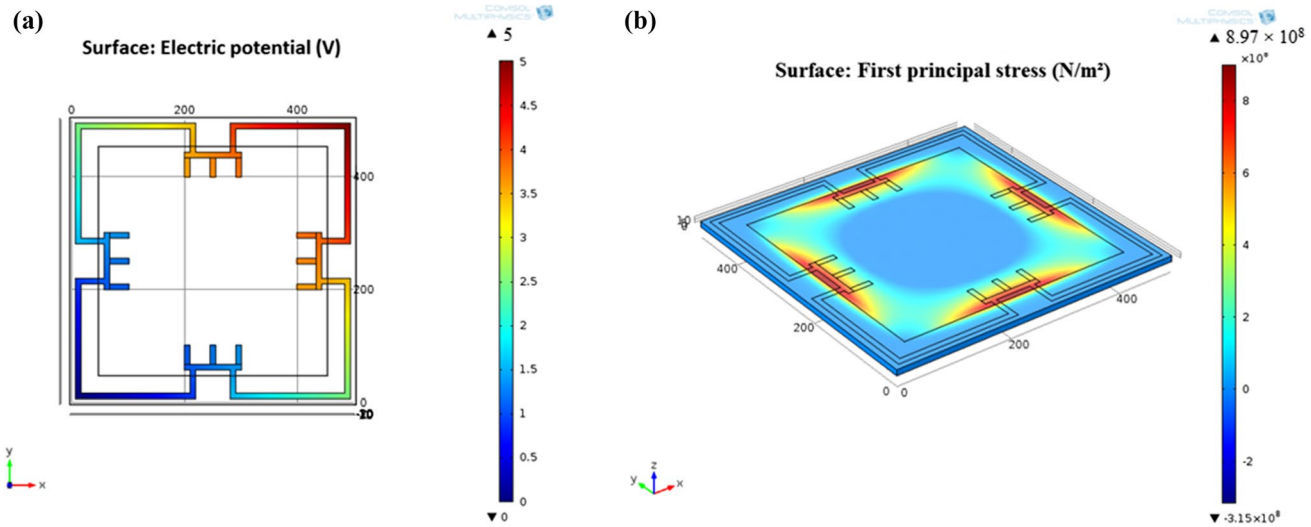


**Fig. 4** Simulation results of Design-1: **a** electric potential (*V*) distribution, **b** stress region of the pressure sensor (Color figure online)

four piezoresistor arms in each side of the diaphragm. This second design is proposed for analyzing the outputs that can be compared with the first design. Figure 5 represents the geometry of the proposed Design-2.

Since the number of the piezoresistor arm is increased in the second design, the length of each piezoresistor arm is taken as 25 µm. This model is also designed in the COMSOL Multiphysics software. All of the steps in design procedure are same as Design-1. Figure 6 represents the simulated result of total displacement at 1 MPa. The deformation of Design-2 sensor is achieved as 2.62 µm at 1 MPa. The displacement of this sensor is also observed for the pressure range of 0 to 5 MPa. However, the maximum displacement is obtained at 20 MPa. Moreover, the electric potential distribution of Design-2 is displayed in Fig. 7a. The simulated output voltage is 13.6 mV to 68 mV for applied pressure of 1 MPa to 5 MPa. Thus, with the increase in the applied pressure, the output voltage is increased. It can be acknowledged that the output voltage of Design-2 is low compared to Design-1. In addition, the maximum stress of $1.07 \times 10^8$ N/m$^2$ is achieved from this model which is denoted by the red region area in Fig. 7b. While comparing the first principle stress of Design-1 and Design-2, Design-1 shows about nine times greater stress. Although Design-1 and Design-2 have similar materials, Design-1 achieved better performance because of less number of piezoresistor arms. The less number of arms enhances piezoresistive effects. Hence, Design-1 is more suitable for application in a highly stressful situation than Design-2. The graphical representation of all outputs is shown in the result analysis section.

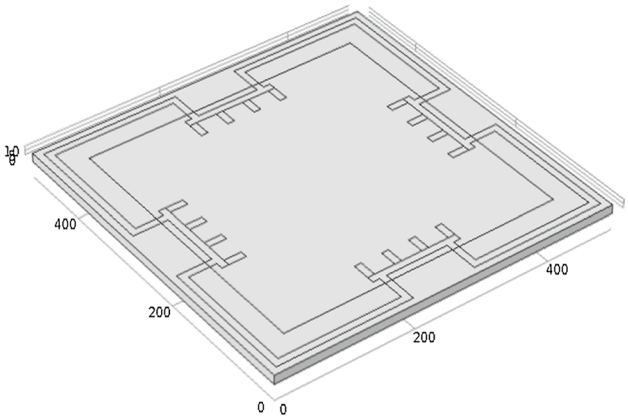


**Fig. 5** Geometry of Design-2

## 5 Result analysis

Various parameters such as deflection of the diaphragm, output voltage, and sensitivity are the analysis characteristics of the proposed models. For the applied pressure of 0 to 5 MPa, the corresponding displacement and the electric potential are computed to get the value of the linearity and the sensitivity. In this section, the simulated and the mathematical results of the linearity and the sensitivity are presented. Figure 8 shows the graph of displacement versus applied pressure for Design-1, Design-2, and the theoretical result. The theoretical values of the displacement are computed from Eq. (3). The reference point for measuring displacement is the center of the diaphragm where the maximum displacement is achieved. It is observed that the displacement of Design-1 is close to the theoretical result. In addition, the output curve of Design-2 is less linear than Design-1. When the pressure increases, the displacement in the sensor also increases. This graph confirms the linearity of the piezoresistive pressure sensor for Design-1.

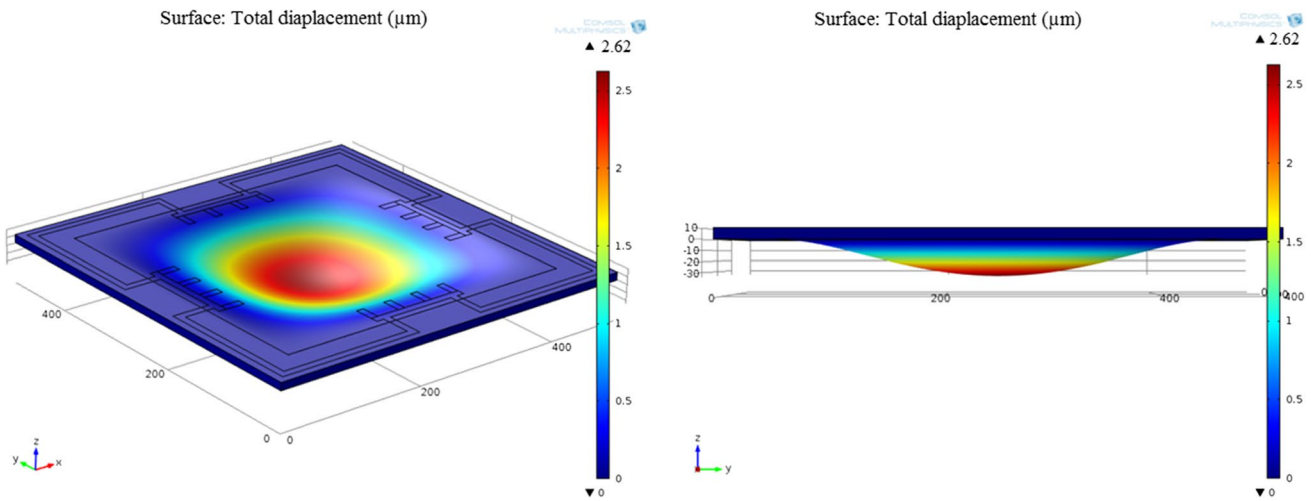


**Fig. 6** 3D simulation results of Design-2: total displacement is in µm range at the applied pressure of 1 MPa

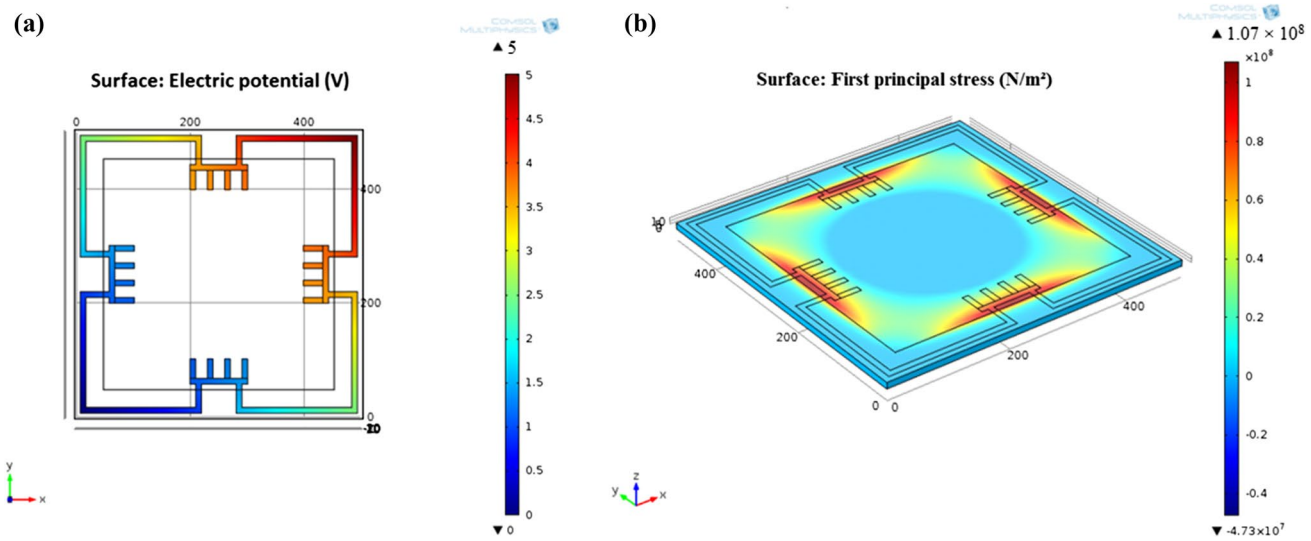


**Fig. 7** Simulation results of Design-2: **a** electric potential (*V*) distribution, **b** stress region of the pressure sensor

**Fig. 8** Displacement versus applied pressure

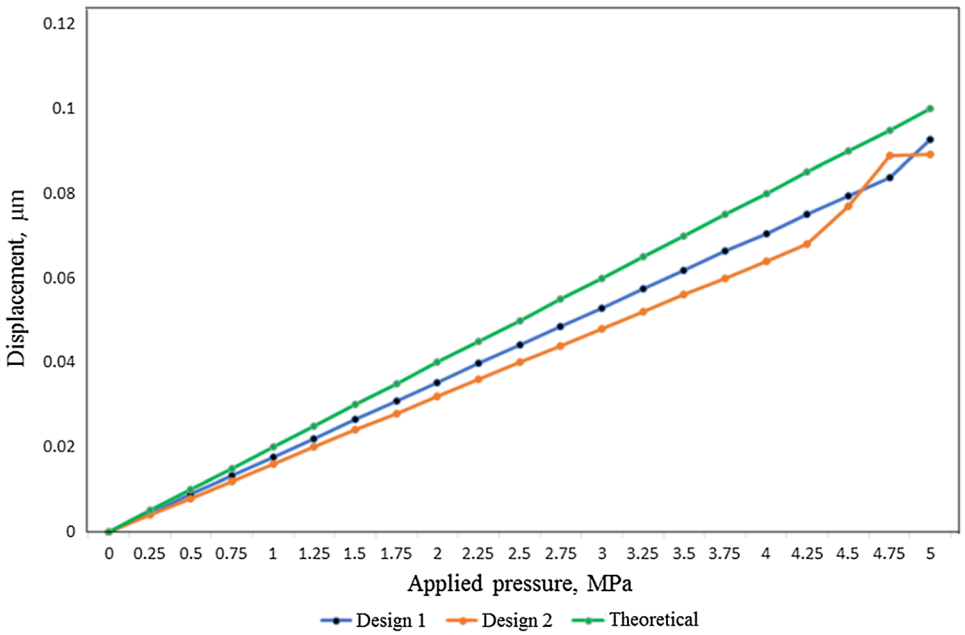


Additionally, Fig. 9 represents the change in the output voltages across the bridge due to the change in applied pressure of Design-1, Design-2, and the theory calculated from Eq. (5). In this graph, it is observed that as the applied pressure increases, the output voltage increases. The output voltages of Design-1 are greater than the output voltages of Design-2. The sensitivity of the piezoresistive pressure sensor can be determined from this plot with the help of Eq. (6). Equation (6) confirms that if the difference in applied pressure is low, then the sensitivity of the sensor is raised. The achieved simulated sensitivity for Design-1 is 7.736 mV/V/MPa and for Design-2 is 2.72 mV/V/MPa. Thus, the measured sensitivity of Design-2 is lower compared to Design-1. Therefore, it can be concluded that the increasing number of piezoresistor arms decrease not only the linearity performance but also the sensitivity of the piezoresistive pressure sensor. Thus, Design-1 shows better sensitivity and linearity.

For further analysis, the proposed Design-1 is simulated with the variations in diaphragm thickness. Table 2 represents the performances of Design-1 for various thicknesses of the sensor. It is indicated that the thicker diaphragm reduces the displacement and the sensitivity. On the contrary, thicker diaphragm makes pressure

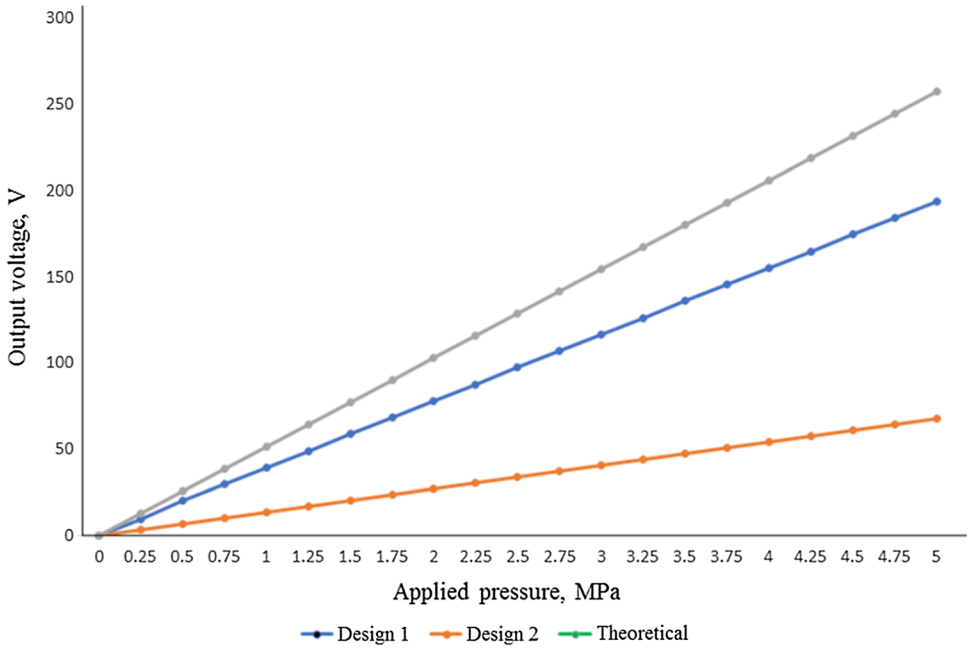


**Fig. 9** Electric potential versus applied pressure

**Table 2** Performances of Design-1 for thickness variations

| Thickness (μm) | Displacement (μm) for 1 MPa | Sensitivity (mV/V/MPa) | Pressure range (MPa) |
|---|---|---|---|
| 5 | 0.032 | 14.4 | 0 to 1 |
| 10 | 0.017 | 7.4 | 0 to 5 |
| 15 | 0.009 | 1.36 | 0 to 20 |
| 20 | 0.0034 | 0.25 | 0 to 35 |

range wider. In addition, although the displacement and sensitivity performance of the sensor are improved for 5 μm thickness, the range of the pressure is very low compared to others. Thus, the trade-off of the displacement, sensitivity, and pressure range of the piezoresistive pressure sensor is needed. The optimum thickness of the diaphragm is 10 μm. Keeping all these considerations, the proposed Design-1 shows the better displacement, sensitivity, and pressure range.

## 6 Comparative analysis and discussions

In this section, the characterization of the existing pressure sensors with their parameters and results are provided and analyzed. Table 3 summarizes the achieved performance of the existing pressure sensors with our proposed designs.

While Katageri and Sheeparamatti's work [12] is compared with Xu et al. [18], it is seen that former paper used carbon nanotube (cnt) as a piezoresistive material whose Young's modulus (1000 GPa) was much higher than the boron oxide used in latter work. As a result, the operable pressure range of Ref. [12] was wider than [18]. The Katageri's [12] sensor operated at highest 1 MPa, whereas only 500 pa of the maximum pressure was used in Ref. [18]. Although the diaphragm size in [18] was nine times greater than that of [12], the Katageri's sensor [12] was operable at a wider range. Moreover, the relative permittivity of cnt of 237.4 was another vital parameter for the above-mentioned results.

Moreover, the pressure range of a sensor designed by Guan et al. [28] is narrower than that of Li et al. [27]. It was also observed from Ref. [27] that the greater thickness increased the pressure range and reduced the sensitivity. On the contrary, the lower thickness in [28] improved the sensitivity and declined the pressure range. As a result, the optimization of the thickness of the diaphragm is a major factor.

Although Sujit et al. [37] used the least size of diaphragm among Guan et al. [28], Li et al. [27], Tran et al. [45], and Xu et al. [18], the pressure range of [37] was wider than those in the above-mentioned studies. It was between 0 and 200 kPa which is around 50 times greater than other pressure ranges. In Ref. [37], the material used for the piezoresistors was polysilicon which made the sensor to operate in a wider range of pressure. However, the pressure range of our proposed design is much wider than Ref. [37]. Though the diaphragm size (400 μm × 400 μm) of the proposed sensor is least among these references, it shows the highest pressure range. Moreover, the stripped-shaped piezoresistors have

**Table 3** Comparison of different parameters and results of some existing works

| References | Material properties | | Results | |
|---|---|---|---|---|
| | Diaphragm | Piezoresistors | Pressure range | Sensitivity |
| Katageri and Sheeparamatti [12] | n-type silicon<br>Dimension = 400 μm × 400 μm<br>Thickness = 10 μm | Carbon nanotube<br>Length = 50 μm | 1 Pa to 1 MPa | 6.02 μV/V/Pa |
| Bannikoppa et al. [11] | n-type silicon<br>Dimension = 400 μm × 400 μm<br>Thickness = 10 μm | p-type silicon<br>Length = 50 μm and 100 μm | 0 to 1 MPa | 2.75 mV/kPa for 100 μm<br>9.27 mV/kPa for 50 μm |
| Guan et al. [28] | Width = 1900 μm<br>Thickness = 16 μm<br>Shuriken-structured | $SiO_2$ | 0 to 3 kpa | 4.72 mV/kPa/V |
| Meti et al. [22] | n-type silicon<br>Dimension = 400 μm × 400 μm<br>Thickness = 10 μm | p-type silicon<br>Length = 50 μm and 100 μm<br>Meander shape | 0 to 1 MPa | 2.36 mV/kPa for 50 μm<br>1.64 mV/kPa for 100 μm |
| Li et al. [27] | n-type silicon<br>Dimension = 4500 μm × 4500 μm<br>Thickness = 300 ± 5 μm | n-type silicon<br>Four-beams-bossed-membrane | 0 to 5 kpa | 4.71 mV/V/kPa |
| Tran et al. [45] | n-type silicon<br>Dimension = 2900 μm × 2900 μm<br>Thickness = 12 μm | p-type silicon<br>Length = 200 μm | 0 to 5 kPa | 25.7 mV/kPa |
| Hong et al. [24] | n-type silicon<br>Dimension = 400 μm × 400 μm<br>Thickness = 10 μm | p-type silicon | 0 to 1 MPa | − 6.02 mV/kpa |
| Sujit et al. [37] | n-type silicon<br>Dimension = 500 μm × 500 μm<br>Thickness = 25 μm | Polysilicon | 0 to 200 kpa | |
| Xu et al. [18] | Polished n-type silicon<br>Dimension = 3500 μm × 3500 μm<br>Thickness = 10 μm | Boron oxide<br>Length = 200 μm | 0 to 500 pa | 0.06 mV/V/Pa |
| Proposed work (Design-1) | n-type silicon<br>Dimension = 400 μm × 400 μm<br>Thickness = 10 μm | p-type silicon<br>Length = 33.3 μm | 0 to 5 MPa | 7.736 mV/V/MPa |
| Proposed work (Design-2) | n-type silicon<br>Dimension = 400 μm × 400 μm<br>Thickness = 10 μm | p-type silicon<br>Length = 25 μm | 0 to 20 MPa | 2.72 mV/V/MPa |

made the pressure range much wider. The pressure range of the proposed Design-1 is 0 to 5 MPa and of the proposed Design-2 is 0 to 20 MPa.

Among the works of Bannikoppa et al. [11], Meti et al. [22], and Hong et al. [24], Ref. [24] shows the least sensitivity, though all of the sensors configurations were almost same. The author in Ref. [24] used an inner diaphragm in the middle of the sensor. Both [11] and [22] references used 50 μm and 100 μm lengths of piezoresistors for comparative analysis. The work in Ref. [11] showed the higher sensitivity because of the shape of the piezoresistors. The shape of the piezoresistors in [22] was meander shape, and they used a metal material (copper) as the connecting arms. This reduced the sensitivity of the piezoresistive pressure sensor. From this comparison, it is also deducted that the increasing length of the piezoresistors has decreased the sensitivity. Apart from this, while comparing with the proposed sensor, Design-1 and Design-2 exhibited higher sensitivity. The reason behind this is the configuration of the proposed piezoresistive pressure sensors. Additionally, silicon material as the connecting arms has a great impact to enhance the sensitivity.

Although the total length of the piezoresistors for both designs is 100 μm similar to [11] and [22], this 100 μm is slotted in 33.3 μm and 25 μm of piezoresistive arms for proposed Design-1 and Design-2, respectively. In proposed Design-2, though the length of the piezoresistive arms has been decreased, the increasing number of the slotted piezoresistive arms has decreased the sensitivity. However, the pressure range of proposed Design-2 is much wider than proposed Design-1 and other mentioned references too. Therefore, the proposed Design-2 can be implemented for those applications where high pressure range is significant rather than sensitivity. On the other hand, the proposed Design-1 is suitable for that condition where both the sensitivity and pressure range are highly significant.

The advantages of this proposed sensor are simple in structure, easy fabrication, high sensitivity, easily available material, excellent linearity, and wider pressure range detection capability. Although the proposed simulated work has various advantages over the existing sensors, its practical implementation is essential to validate its performance in real-life situation. However, similar types of sensors have been implemented, evaluated, and applied for medical application and high temperature applications in Refs. [18, 45, 46]. Thus, our proposed sensors can be fabricated with existing MEMS compatible fabrication process.

## 7 Conclusion

This work was conducted to find the best combinations of designs to achieve moderate sensitivity within a large range of applied pressure. From our analysis and discussion, it can be deduced that the n-silicon (single crystal) diaphragm, p-silicon (single crystal) piezoresistor combination, and the stripped-shaped design enhance the performance of the piezoresistive pressure sensor. This combination gives a better sensitivity within a wider range. This MEMS-based piezoresistive pressure sensor was designed and simulated using the COMSOL Multiphysics tool. The deflection of the diaphragm was analyzed according to the applied pressure. As the pressure was increased, the output voltage across the Wheatstone bridge was also increased. The paper presented two different designs and simulations of piezoresistive micro-pressure sensors which were operated over a higher pressure range. Analyzing those two designs, Design-1 achieved a good sensitivity of 7.736 mV/V/MPa and better performance over the range of 0–5 MPa. The sensitivity of the sensor can also be increased by decreasing the thickness of the diaphragm and by changing the other parameters. For future enhancement of the sensitivity, a SOI (silicon on insulator) layer can be introduced where a sandwich layer of silicon–insulator–silicon layer can be used.

## References

1. Pramanik, C., Saha, H., Gangopadhyay, U.: Design optimization of a high performance silicon MEMS piezoresistive pressure sensor for biomedical applications. J. Micromech. Microeng. **16**, 2060–2066 (2006). https://doi.org/10.1088/0960-1317/16/10/019
2. Ansermet, S., Otter, D., Craddock, R.W., Dancaster, J.L.: Cooperative development of a piezoresistive pressure sensor with integrated signal conditioning for automotive and industrial applications. Sens. Actuators, A **21**(1–3), 79–83 (1990). https://doi.org/10.1016/0924-4247(90)85016-W
3. Lin, L., Yun, W.: MEMS pressure sensors for aerospace applications. IEEE Aerosp. Conf. Proc. **1**, 429–436 (1998). https://doi.org/10.1109/AERO.1998.686941
4. Aravamudhan, S., Bhansali, S.: Reinforced piezoresistive pressure sensor for ocean depth measurements. Sens. Actuators, A **142**(1), 111–117 (2008). https://doi.org/10.1016/j.sna.2007.04.036
5. Je, C.H., Lee, S.Q., Yang, W.S.: High sensitivity surface micromachined absolute pressure sensor. Proc. Eng. **168**, 725–728 (2016). https://doi.org/10.1016/j.proeng.2016.11.261
6. Jornod, A., Rudolf, F.: High-precision capacitative absolute pressure sensor. Sens. Actuators **17**(3–4), 415–421 (1989). https://doi.org/10.1016/0250-6874(89)80028-9
7. Matsuoka, Y., Yamamoto, Y., Tobita, T., Shimada, S., Yasukawa, A.: Design method for sensing body of differential pressure transmitter using silicon diaphragm-type pressure sensor. IEEE Trans. Instrum. Meas. **44**(3), 791–794 (1995). https://doi.org/10.1109/19.387334
8. Mastrangelo, C.H., Zhang, X., Tang, W.C.: Surface-micromachined capacitive differential pressure sensor with lithographically defined silicon diaphragm. J. Microelectromech. Syst. **5**(2), 98–105 (1996). https://doi.org/10.1109/84.506197
9. Moe, S.T., Schjølberg-Henriksen, K., Wang, D.T., Lund, E., Nysæther, J., Furuberg, L., Visser, M., Fallet, T., Bernstein, R.W.: Capacitive differential pressure sensor for harsh environments. Sens. Actuators, A **83**(1–3), 30–33 (2000). https://doi.org/10.1016/S0924-4247(99)00374-X
10. Pang, C., Lee, G.Y., Kim, T.I., Kim, S.M., Kim, H.N., Ahn, S.H., Suh, K.Y.: A flexible and highly sensitive strain-gauge sensor using reversible interlocking of nanofibers. Nat. Mater. **11**(9), 795 (2012). https://doi.org/10.1038/nmat3380
11. Bannikoppa, S., Katageri, A.C., Balavalad, K.B., Sheeparamatti, B.G.: Design of piezoresistive pressure sensor for enhanced sensitivity. In: 2016 International Conference on Energy Efficient Technologies for Sustainability, pp. 706–710 (2016). https://doi.org/10.1109/ICEETS.2016.7583841
12. Katageri, A.C., Sheeparamatti, B.G.: Design and simulation of carbon nanotube based piezoresistive pressure sensor for patient monitoring application. In: Eighth ISSS National Conference on MEMS, Smart Materials, Structures and Systems (2016)
13. Hassani, A., Skorobogatiy, M.: Design of the microstructured optical fiber-based surface plasmon resonance sensors with enhanced microfluidics. Opt. Express **14**(24), 11616–11621 (2006). https://doi.org/10.1364/OE.14.011616
14. Buckle, P.E., Davies, R.J., Kinning, T., Yeung, D., Edwards, P.R., Pollard-Knight, D., Lowe, C.R.: The resonant mirror: a novel optical sensor for direct sensing of biomolecular interactions part II: applications. Biosens. Bioelectron. **8**(7–8), 355–363 (1993). https://doi.org/10.1016/0956-5663(93)80074-Y
15. Van Herwaarden, A.W., Sarro, P.M.: Thermal sensors based on the seebeck effect. Sens. Actuators **10**(3–4), 321–346 (1986). https://doi.org/10.1016/0250-6874(86)80053-1
16. Lai, J., Perazzo, T., Shi, Z., Majumdar, A.: Optimization and performance of high-resolution micro-optomechanical thermal sensors. Sens. Actuators, A **58**(2), 113–119 (1997). https://doi.org/10.1016/S0924-4247(96)01401-X
17. Rahman, S.H.A., Soin, N., Ibrahim, F.: Residual stress of graphene-based MEMS ICP piezoresistive pressure sensors. In: 2016 International Conference on Bioengineering for Smart Technologies, pp. 1–4 (2016). https://doi.org/10.1109/BIOSMART.2016.7835469
18. Xu, T., Wang, H., Xia, Y., Zhao, Z., Huang, M., Wang, J., Zhao, L., Zhao, Y., Jiang, Z.: Piezoresistive pressure sensor with high sensitivity for medical application using peninsula-island structure. Front. Mech. Eng. **12**(4), 546–553 (2017). https://doi.org/10.1007/s11465-017-0447-9
19. Riedl, X., Bolzmacher, C., Wagner, R., Bauer, K., Schwesinger, N.: A novel PDMS based capacitive pressure sensor. In: 2010 IEEE Sensors, pp. 2255-2258 (2010). https://doi.org/10.1109/ICSENS.2010.5690709

20. Akar, O., Akin, T., Najafi, K.: A wireless batch sealed absolute capacitive pressure sensor. Sens. Actuators, A **95**(1), 29–38 (2001). https://doi.org/10.1016/S0924-4247(01)00753-1
21. Foland, S., Swedlove, B., Nguyen, H., Lee, J.B.: One-dimensional nanograting-based guided-mode resonance pressure sensor. J. Microelectromech. Syst. **21**(5), 1117–1123 (2012). https://doi.org/10.1109/JMEMS.2012.2203792
22. Meti, S., Balavalad, K.B., Katageri, A.C., Sheeparamatti, B.G.: Sensitivity enhancement of piezoresistive pressure sensor with meander shape piezoresistor. In: 2016 International Conference on Energy Efficient Technologies for Sustainability, pp. 890–895 (2016). https://doi.org/10.1109/ICEETS.2016.7583874
23. Lin, L., Chu, H.C., Lu, Y.W.: A simulation program for the sensitivity and linearity of piezoresistive pressure sensors. J. Microelectromech. Syst. **8**(4), 514–522 (1999). https://doi.org/10.1109/84.809067
24. Hong, C.K., Ismail, N.F., Yunus, N.A.M., Ahmad, D.: Sensitivity of piezoresistive pressure sensor with inner diaphragm. In: 2017 IEEE Asia Pacific Conference on Postgraduate Research in Microelectronics and Electronics, pp. 129–132 (2017). https://doi.org/10.1109/PRIMEASIA.2017.8280381
25. Meti, S., Balavalad, K., Sheeparamatti, B.G.: Sensitivity analysis of silicon based micro pressure sensors using different configurations of meander shape piezoresistors. Int. J. Eng. Sci. Comput. **6**, 6241–6245 (2016). https://doi.org/10.4010/2016.1506
26. Zhu, S.E., Krishna Ghatkesar, M., Zhang, C., Janssen, G.C.A.M.: Graphene based piezoresistive pressure sensor. Appl. Phys. Lett. **102**(16), 161904 (2013). https://doi.org/10.1063/1.4802799
27. Li, C., Ocaña, J.L.: The design of a novel structural four-beams-bossed-membrane (FBBM) piezoresistive pressure sensor. In: 2017 Spanish Conference on Electron Devices, pp. 1–4 (2017). https://doi.org/10.1109/CDE.2017.7905226
28. Guan, T., Yang, F., Wang, W., Huang, X., Jiang, B., He, J., Zhang, L., Fu, F., Li, D., Li, R., Zhao, Q.: A novel 0–3 kPa piezoresistive pressure sensor based on a Shuriken-structured diaphragm. In: 2016 IEEE 29th International Conference on Microelectromechanical Systems, pp. 816–819 (2016). https://doi.org/10.1109/MEMSYS.2016.7421754
29. Meti, S., Balavald, K.B., Sheeparmatti, B.G.: MEMS piezoresistive pressure sensor: a survey. Int. J. Eng. Res. Appl. **6**(4 part 1), 23–31 (2016)
30. Mosser, V., Suski, J., Goss, J., Obermeier, E.: Piezoresistive pressure sensors based on polycrystalline silicon. Sens. Actuators, A **28**(2), 113–132 (1991). https://doi.org/10.1016/0924-4247(91)85020-O
31. Wu, C.H., Zorman, C.A., Mehregany, M.: Fabrication and testing of bulk micromachined silicon carbide piezoresistive pressure sensors for high temperature applications. IEEE Sens. J. **6**(2), 316–324 (2006). https://doi.org/10.1109/JSEN.2006.870145
32. Wu, C.H., Stefanescu, S., Kuo, H.I., Zorman, C.A., Mehregany, M.: Fabrication and testing of single crystalline 3C-SiC piezoresistive pressure sensors. In: Transducers'01 Eurosensors XV, pp. 514–517 (2001). https://doi.org/10.1007/978-3-642-59497-7_122
33. Pallas-Areny, R., Webster, J.G.: Sensors and Signal Conditioning. Wiley, New York (2012)
34. Fraden, J.: Handbook of Modern Sensors: Physics, Designs, and Applications. Springer, Berlin (2004)
35. Reverter Cubarsí, F., Horak, G., Bilas, V., Gasulla Forner, M.: Novel and low-cost temperature compensation technique for piezoresistive pressure sensors. In: XIX IMEKO World Congress. Fundamental and Applied Metrology, pp. 2084–2087 (2009)
36. Bhat, K.N., Nayak, M.M.: MEMS pressure sensors-an overview of challenges in technology and packaging. J. Smart Struct. Syst. **2**, 1–10 (2013)
37. Sujit, E.S., Kusuma, N., Hemalatha, B.: Polysilicon piezoresistive MEMS pressure sensor: study of analytical solutions for diaphragm and design & simulation. In: 2017 International Conference on Communication and Signal Processing, pp. 1606–1610 (2017). https://doi.org/10.1109/ICCSP.2017.8286660
38. Kumar, S.S., Ojha, A.K., Nambisan, R., Sharma, A.K., Pant, B.D.: Design and simulation of MEMS silicon piezoresistive pressure sensor for barometric applications. In: Proceedings of the ARTCom&ARTEE PEIE&itSIP and PCIE, pp. 339–345 (2013)
39. Rashidi, F.R.M., Hussein, O., Hasan, W.Z.W.: Investigation on developing of a piezoresistive pressure sensor for foot plantar measurement system. In: 2015 IEEE Regional Symposium on Micro Nanoelectronics (RSM), pp. 1–4 (2015). https://doi.org/10.1109/RSM.2015.7354969
40. Balavalad, K.B., Sheeparamatti, B.G.: Design simulation and analysis of piezoresistive micro pressure sensor for pressure range of 0 to 1 MPa. In: 2016 International Conference on Electrical, Electronics, Communication, Computer and Optimization Techniques, pp. 345–349 (2016). https://doi.org/10.1109/ICEECCOT.2016.7955243
41. Herrera-May, A.L., Soto-Cruz, B.S., López-Huerta, F., Aguilera Cortés, L.A.: Electromechanical analysis of a piezoresistive pressure microsensor for low-pressure biomedical applications. Rev. Mex. Fís. **55**(1), 14–24 (2009)
42. Hegde, V., Veena, S., Ravikumar, H.M., Yellampalli, S.: Piezoelectric acoustic pressure sensor diaphragm design for energy harvesting. In: 2014 International Conference on Advances in Energy Conversion Technologies, pp. 21–26 (2014). https://doi.org/10.1109/ICAECT.2014.6757055
43. Nemeth, N.N., Jadaan, O., Palko, J.L., Mitchell, J.S., Zorman, C.A.: Structural modeling and probabilistic characterization of MEMS pressure sensor membranes. In: MEMS: Mechanics and Measurements, Society of Experimental Mechanics Symposium, p. 46 (2001)
44. Madduri, N.J., Lakkoju, G., Kasturi, B.L., Sravanam, S., Satyanarayana, T.: Design and deformation analysis of MEMS based piezoresistive pressure sensor. Int. J. Adv. Eng. Technol. **7**(2), 521 (2014). https://doi.org/10.1016/j.matpr.2017.11.291
45. Tran, A.V., Zhang, X., Zhu, B.: The development of a new piezoresistive pressure sensor for low pressures. IEEE Trans. Ind. Electron. **65**(8), 6487–6496 (2017). https://doi.org/10.1109/TIE.2017.2784341
46. Tran, A.V., Zhang, X., Zhu, B.: Effects of temperature and residual stresses on the output characteristics of a piezoresistive pressure sensor. IEEE Access **7**, 27668–27676 (2019). https://doi.org/10.1109/ACCESS.2019.2901846